



CrossMark  
click for updates

Cite this: *RSC Adv.*, 2016, 6, 24865

# Interfacial separation and electrochemical delamination of CVD grown multilayer graphene for recyclable use of Cu powder

Zhuo Wang,<sup>ab</sup> Zhihong Liu,<sup>a</sup> Mahmuda Akter Monne,<sup>a</sup> Shuangyue Wang,<sup>ac</sup> Qingkai Yu<sup>a</sup> and Maggie Yihong Chen<sup>\*a</sup>

This paper demonstrates a simple and repeatable method to produce multilayer graphene by chemical vapor deposition (CVD) growth and nondestructive electrochemical delamination from Cu powder. SEM images show that Cu powder with graphene isolated by graphite is free from sintering and could be separated by the water/hexane interface with ultrasonication. The graphene peeled by electrochemical delamination composing multilayer carbon atom sheets (<5 layers) is characterized by Raman spectra and AFM images. This method is scalable, and the Cu powder is reusable in multiple growth and delamination cycles.

Received 6th November 2015  
Accepted 22nd February 2016

DOI: 10.1039/c5ra23360g

[www.rsc.org/advances](http://www.rsc.org/advances)

## Introduction

Graphene, a single sheet composed of sp<sup>2</sup> hybridized carbon, as the next generation semiconductor material for post-silicon electronics, has drawn considerable attentions because of its outstanding electronic, optical, thermal, and mechanical properties.<sup>1–3</sup> Generally, large-scale production approaches of graphene for widespread applications include growth by chemical vapor deposition (CVD) on metal substrates;<sup>4a,b</sup> segregation by heat treatment of silicon carbide;<sup>5</sup> and liquid-phase exfoliation (LPE).<sup>6</sup>

The liquid-phase production of chemically converted graphene from graphene oxide is a high-yield method for monolayer graphene.<sup>7,8</sup> However, a substantial number of defects are introduced during the reduction process and the intrinsic properties of graphene are only partially restored.<sup>9</sup> Alternatively, graphene with absence of defects or oxides produced by dispersion and exfoliation of graphite in organic solvents is reported, and this method results in a monolayer yield of ~1 wt%. The XPS spectrum of liquid-phase exfoliated graphene shows that ~11 wt% residual NMP (*N*-methyl-pyrrolidone) after drying at room temperature at  $\sim 1 \times 10^{-3}$  mbar, even after a subsequent vacuum anneal at 400 °C.<sup>10</sup> Also, graphene with low defects could be delaminated from graphite with microwave treatment and interaction with the surfactant cetyltrimethylammonium

bromide (CTAB) in aqueous solution.<sup>11</sup> The CTAB intercalation in graphite has achieved the delamination but the molecule of surfactant absorbed on the surface of graphene would be not good for further applications.

The most promising, inexpensive, and readily accessible approach for deposition of reasonably high-quality graphene is CVD onto metal substrates such as Ni and Cu.<sup>4a,b</sup> Based on the large surface areas of metal micro-/nano-particles, graphene flakes could be CVD grown and delaminated in mass production. Typically, the growth temperature of graphene on Cu is about 1000 °C, which is close to or even above the melting point of Cu particles (according to the particle size).<sup>12</sup> Therefore, sintering between contact Cu particles will increase dramatically to reduce the surface area, and few Cu particles could be repeatable as substrate for CVD growth. Additionally, conventional methods of delaminating graphene from metal substrates usually include a chemical etching step to remove the metal.<sup>13</sup> The etching step not only increases the production cost and requires a long treatment of several hours but also consumes the Cu particle for recycling use. A nondestructive bubble-aid transfer method has been developed to peel the graphene films from metal substrate (Cu, Pt, *etc.*) in electrochemical delamination process.<sup>14,15</sup>

In our work, graphite powder is used to isolate Cu powder from sintering in the CVD process. Graphene-coated Cu powder is separated efficiently from the mixture product by interface of immiscible liquid, and multilayer graphene is peeled nondestructively by electrochemical delamination. Our method demonstrates a potential way of producing graphene powder characterized with simple and low-cost reusability of the Cu and graphite powders in multiple growth and delamination cycles, which will work for continuous mass production.

<sup>a</sup>Ingram School of Engineering, Texas State University-San Marcos, 601 University Dr., San Marcos, TX, 78666, USA. E-mail: yc12@txstate.edu

<sup>b</sup>School of Material Science and Engineering, Chang'an University, No. 65 North Chang'an Road, Xi'an, 710061, P. R. China

<sup>c</sup>Institute of Fundamental and Frontier Sciences and School of Physical Electronics, University of Electronic Science and Technology of China, Chengdu, 610054, P. R. China

## Experimental procedure

All of the chemicals in our experiment are used as received without further treatments.

### CVD growth of graphene

The graphene is grown by the atmospheric pressure CVD method. A homemade CVD system consisting of an MTI OTF-1200X-3 furnace and MKS mass flow controllers is used in the experiment. A mixture of Cu powder (spherical APS 10  $\mu\text{m}$  99.9% metal basis, Alfa Aesar) and graphite powder (crystalline 300 mesh 99%, Alfa Aesar) with a weight ratio of 1 : 2 as the starting materials is loaded into the furnace and heated up to 1050  $^{\circ}\text{C}$  under 300 sccm Ar and 20 sccm  $\text{H}_2$ . After reaching 1050  $^{\circ}\text{C}$ , the sample is annealed for 30 minutes without changing the gas flow rate. We then switch the gas to 20 sccm  $\text{H}_2$ , 300 sccm  $\text{CH}_4$  (476 ppm diluted in Ar) and grow for 30 minutes. The sample is cooled to room temperature in the furnace with 300 sccm Ar and 20 sccm  $\text{H}_2$ .

### Separation

Hexane is poured onto DI water to form an immiscible interface. The obtained product mixture is added into the water/hexane system with ultrasonication. The dispersion is standing until no Tyndall effect is detected in the water section. The precipitated red Cu powder is collected and washed with DI water. The interface-trapped black graphite powder is also collected and washed for recycling.

### Electrochemical delamination of CVD-grown graphene from Cu powder

The separated red powder is placed into a bowl structure Cu electrode. Pt is used as the counter electrode in the system. The electrolyte of sodium hydroxide (NaOH) solution with a concentration of 0.25 M is added carefully by pipette to submerge the bowl without causing turbulence in the liquid. The hexane is added on the top of electrolyte by drops. The voltage applied is increased to the stage of bubble appearance on electrodes and maintained. The corresponding electrolytic voltage is usually 3–5 V. After electrochemical delamination, a further ultrasonication treatment on the electrolyte solution is applied, and the floating graphene powders trapped at the hexane/electrolyte interface are collected (silicon wafer is used in our work) by a dip-coating process and washed with DI water to remove NaOH residues. The rest of the Cu powders are collected for recyclable usage. The schematic diagram of electrochemical delamination is shown in Fig. 1.

### Characterization

The microstructures of Cu powder before and after electrochemical delamination are observed by SEM (Nova, NanoSEM, FEI, USA). The quality of obtained graphene is illustrated by Raman spectrum ( $\lambda = 532 \text{ nm}$ ) (DXR Raman microscope, Thermo Scientific, USA). The topology profiles of graphene are observed by AFM (XE-7, Park Systems Inc, Korea).

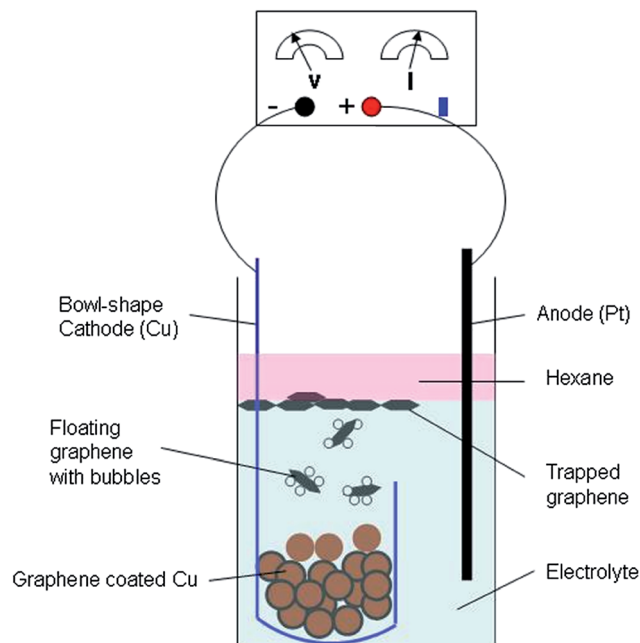


Fig. 1 Schematic diagram of electrochemical cell used for the electrochemical delamination of graphene-coated Cu powder.

## Results and discussion

Generally, the melting temperature of Cu is 1084.62  $^{\circ}\text{C}$  in bulk and is lower with the Cu particle size decreasing. The growth temperature of graphene on Cu micro-powder is 1050  $^{\circ}\text{C}$  in our study, which could enhance the sintering between micron-scale Cu particles. Therefore, graphite micro-powder is mixed with Cu powder to isolate neighbor Cu particles and prevent the possible sintering occurring at contacting areas. The separation of CVD-grown graphene-coated Cu powder from graphite is based on surface energy and density instead of wetting property. The intrinsic wetting behavior of Cu surface is not disrupted significantly by the coating graphene. With an increasing number of graphene layers, the contact angle of water on Cu (85.9 $^{\circ}$ ) gradually transitions towards the bulk graphite value (90.6 $^{\circ}$ ), which is reached for  $\sim 6$  graphene layers.<sup>16</sup> The slight difference of contact angles for graphene-coated Cu and graphite is not selective enough to enforce the separation of the mixture product in pure DI water. As shown in Fig. 2(a), dispersion of mixture is obtained after ultrasonication without obvious separation. Considering matching surface energy of graphite ( $\sim 70\text{--}80 \text{ mJ m}^{-2}$ ) and polarized solvent, good solvents with surface tension within the range of 40–50  $\text{mJ m}^{-2}$  meets the requirement of close-to-zero enthalpy of mixing for graphite dispersed.<sup>17</sup> The surface tension of water and hexane at 20  $^{\circ}\text{C}$  is 72.9  $\text{mJ m}^{-2}$  and 18.4  $\text{mJ m}^{-2}$  respectively, therefore, immiscible liquid interface of water/hexane is qualified and could trap graphite, since its interfacial tension is 50  $\text{mJ m}^{-2}$  and the spreading parameter value is positive with a value of  $\sim 6 \text{ mN m}^{-1}$ .<sup>18</sup> The capillary force at the hexane/water interface is substantially stronger than the gravitational force to hold graphene-coated Cu and graphite as long as the thickness of

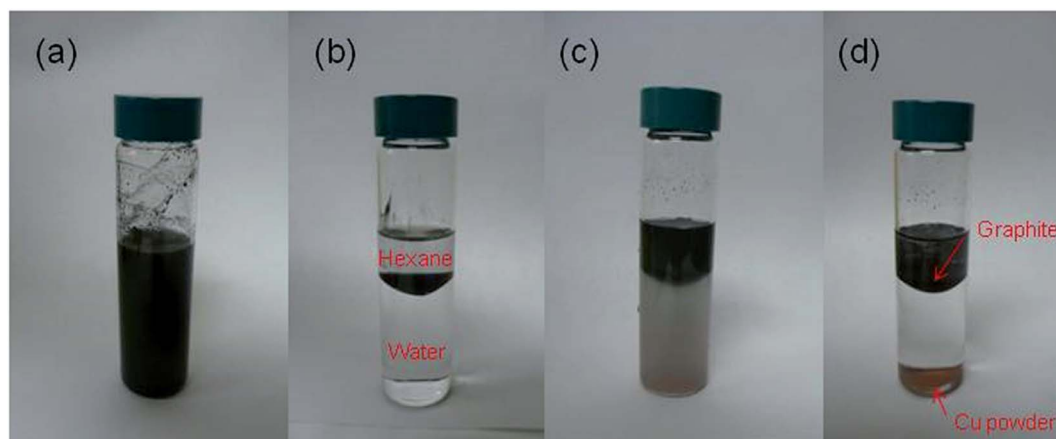


Fig. 2 (a) Dispersion of mixture powder in DI water; (b) mixture powder is trapped at the water/hexane interface; (c) dispersions of Cu powder in DI water and graphite powder in hexane after ultrasonication; (d) separated mixture powder after long-time precipitation.

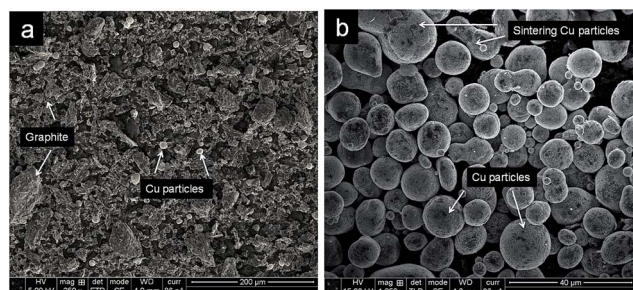


Fig. 3 (a) The mixture of Cu powder and graphite after CVD growth; (b) the Cu powder with CVD-grown graphene after interfacial separation.

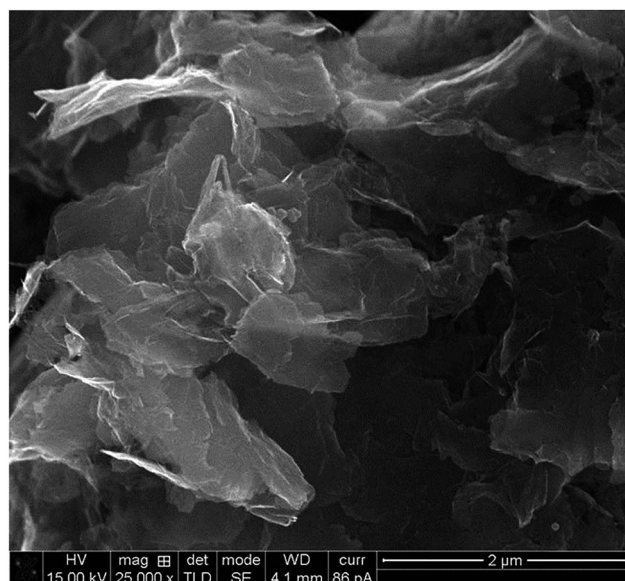


Fig. 5 The delaminated graphene collected from the hexane/electrolyte interface.

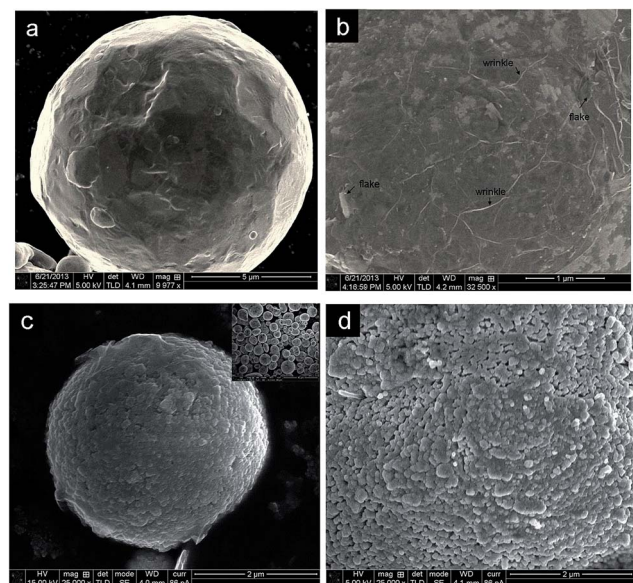


Fig. 4 (a) Cu particle after CVD growth; (b) CVD-grown graphene on the surface of a Cu particle; (c) the morphology of the Cu particle and (d) the detail of the Cu surface after electrochemical delamination.

floating powder is thinner than the capillary length of 1.2 mm,<sup>19</sup> as shown in Fig. 2(b). Cone-shape interface originates from the balance of capillary and gravity, and no Cu particles are separated from the interface caused by the difference in density.

In the process of ultrasonication, acoustic cavitation could help generate a small droplet, and an immiscible dispersion of hexane in water is acquired.<sup>20</sup> Based on the surface tensions (water and hexane); frequency of ultrasonication (40 kHz of lab ultrasonic cleaner); and the wetting property of graphite (graphene), the distribution of droplet size is in the range of ~1–10 μm,<sup>21–23</sup> which is in the same range of Cu particles. Therefore, the graphite powder instead of graphene-coated Cu particles will absorb at the interface of hexane droplets for the consideration of geometric shape (the Cu particle and hexane droplet are sphere shaped with the same dimension, but graphite



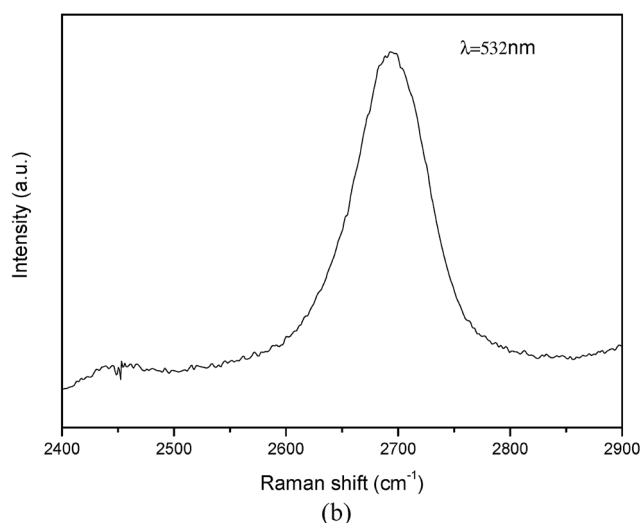
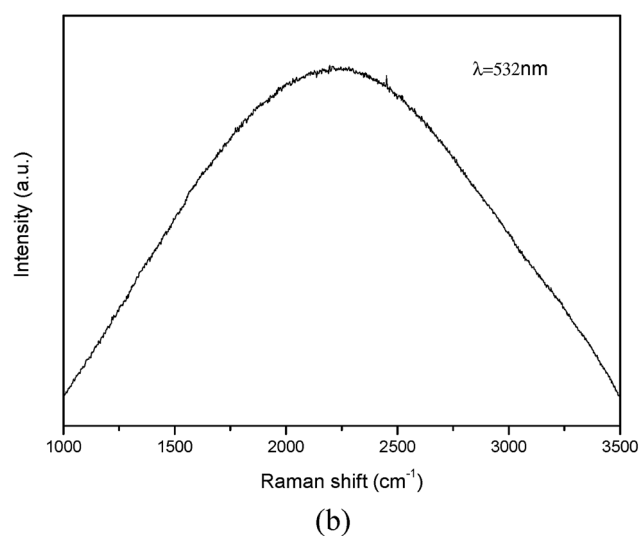
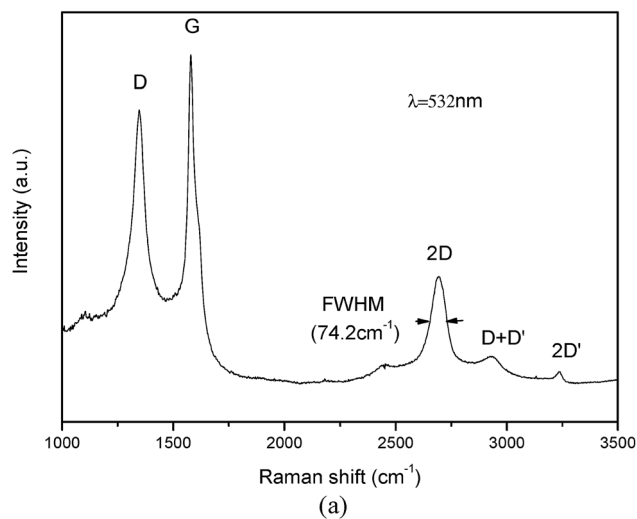
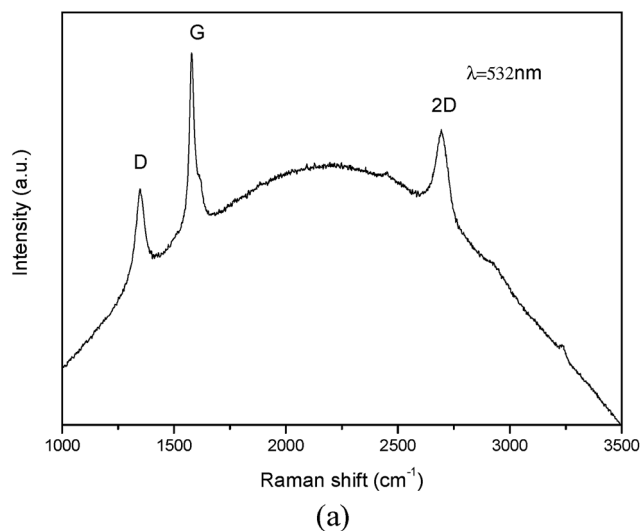


Fig. 6 Raman spectra (excitation wavelength  $\lambda = 532$  nm) for (a) Cu powder with graphene after interfacial separation; (b) Cu powder after electrochemical delamination.

Fig. 7 Raman spectra (excitation wavelength  $\lambda = 532$  nm) for (a) delaminated graphene flakes; (b) 2D Raman spectra.

powder is amorphous with a wide distribution of size, as shown in Fig. 3(a)) and surface energy of graphite to minimize of the Helmholtz free energy.<sup>23</sup> The droplets could not be stabilized completely by the absorbed graphite on the interface because the size of graphite particles is also comparable with the droplet. The absorbed graphite powder will float to the surface of water with dispersed hexane droplets and collect at the immiscible liquid interface after re-coalescence of droplets to the continuous phase of hexane. Although the Cu particles are coated with multilayer graphene sharing the same wetting property of graphite, the difference in density of Cu ( $8.96 \text{ g cm}^{-3}$ ) and graphite ( $2.09\text{--}2.33 \text{ g cm}^{-3}$ ) will dominate the separation because the buoyant force of floating hexane droplets is not strong enough to balance the gravity of Cu but it is enough for graphite. Fig. 2(c) and (d) show the dispersions of Cu in water (red) and graphite in hexane (black) by ultrasonication before and after a longtime precipitation. The graphite powder

is trapped at the water/hexane interface, and Cu powder is collected as sediment.

After interfacial separation, Cu powders are completely separated from graphite powder, as Fig. 3(b) shows. Few Cu particles with a sintered “neck” could be observed to confirm the graphite isolating the Cu particles from sintering. But a simple mechanical mixing of graphite and Cu powders is not absolutely homogenous, and random contacts between neighbor particles are occurring.

An isolated Cu particle after CVD growth is shown in Fig. 4(a). A higher-resolution image of graphene on Cu surface shows the net of “wrinkle” and non-uniform graphene flakes (black arrows) in Fig. 4(b). “Wrinkles” associated with the thermal expansion coefficient difference between Cu and graphene could act to release stress, which indicates that the CVD-grown graphene on the surface of Cu powders is continuous.<sup>4b</sup> Non-uniform graphene flakes originate from the multi-nucleation on the surface of Cu particles or nucleation at contact areas with nearby graphite.

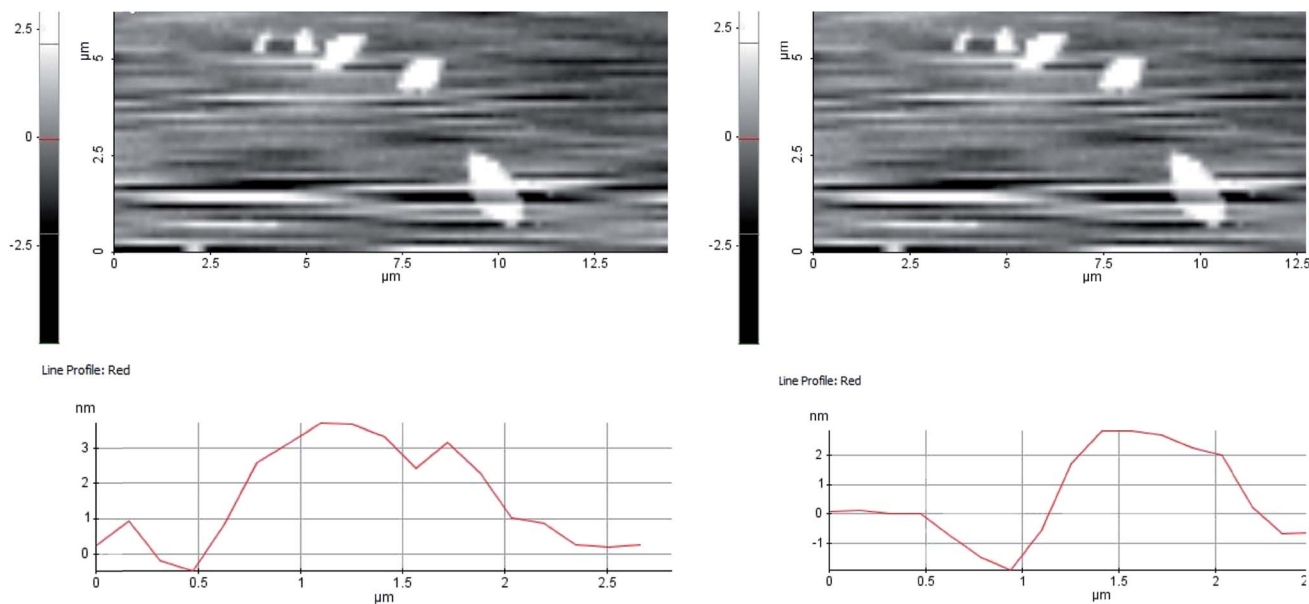


Fig. 8 AFM image of graphene flakes on silicon wafer and height profiles.

The electrochemical delamination has been reported as an effective method to peel off graphene film from Cu or Pt foil.<sup>14,15</sup> Generally, PMMA is spin-coated to strengthen graphene film in wet-transfer process. After voltage is applied, bubbles generated on metal surface and underneath graphene aid the delamination. The peeled graphene/PMMA film floating on the surface of electrolyte is transferred to target substrate. Metal substrate could be recycled for further CVD growth of graphene. After PMMA film has been washed away, clean graphene is obtained. However, after washing the residual contaminants on graphene from PMMA is still a tough problem.<sup>24</sup> In our work, graphene-coated Cu powder was piled in bowl-like cathode. During electrochemical process, Cu particles are connected electronically by surface contact (graphene) because no PMMA is used, which would isolate graphene-coated Cu particles. A large number of micro-bubbles are generated to aid graphene detaching from the Cu surface.<sup>14</sup> The peeled graphene as well as Cu powder will be floating with bubbles and trapped at the liquid interface, and an ultrasonication is applied to separate the delaminated graphene and Cu powder. Fig. 5 shows the delaminated graphene collected at the hexane/electrolyte interface. After electrochemical delamination, the Cu particle keeps its shape, and no obvious changes are observed, as shown in Fig. 4(c), which includes zoomed-in and zoomed-out images. However, the roughness of the particle surface increase for the Cu powder in a bowl-like cathode will slightly dissolve during electrochemical delamination, as shown in Fig. 4(d). The change of surface morphology is acceptable and has no effect on the reusability of the Cu powder in multiple growths because the nanoscale roughness<sup>4b</sup> will be smoothed near melting temperature of Cu in CVD process.

Raman spectroscopy is used to evaluate the electrochemical delamination process before and after peeling graphene from Cu particle, as shown in Fig. 6(a) and (b), respectively. Three

peaks are corresponding to D, G, and 2D bands of typical graphene with a background signal of Cu. After delamination, no peaks corresponded to graphene could be detected from Cu particles. It means no residues of graphene flakes left on Cu surface, which has been proved in the SEM images in Fig. 4(c) and (d).

Raman spectra of delaminated graphene are shown in Fig. 7. The D peak is due to the breathing modes of  $sp^2$  atoms and requires a defect for activation. Defects induce a significant increase of the D and D' intensities and the decrease of the 2D peak height and broadening. The full width at half maximum (FWHM) of the 2D peak is  $74.2\text{ cm}^{-1}$  in our work, compared to  $32.4\text{ cm}^{-1}$  as reported in ref. 25. As shown in the SEM image in Fig. 4, graphene flakes are  $0.5\text{--}2\text{ }\mu\text{m}$  in diameter. Since the laser spot size in our study is  $1.1\text{ }\mu\text{m}$ , there will always be a large quantity of edges seen by the beam. The lack of broadening of the G peak confirms that the D peak comes from edges and not from diffuse structural disorder in the samples.<sup>10</sup> The D band at  $1347\text{ cm}^{-1}$  in our sample is near the  $D_1$  band at the edge of single-layer graphene. Typically, a further decrease in layers leads to a significant increase in the relative intensity of lower frequency  $D_1$  peak. Also, the evolution of the 2D band as a function of layers presents a decreasing of symmetry at the lower frequency side and an up-shifting of the 2D peak with the increasing number of layers. A near-symmetric 2D band centered at  $\sim 2693\text{ cm}^{-1}$  presented in Raman spectra in Fig. 7(b) indicates that multilayer ( $<5$  layers) graphene is obtained by CVD growth after electrochemical delamination in our study.<sup>26,27</sup>

AFM images of graphene flakes are demonstrated in Fig. 8. The topology profiles show that the average height of our graphene flakes is  $\sim 4\text{ nm}$ . Strano *et al.*<sup>28</sup> reported that the average height of monolayer graphene obtained in solution is  $1.7\text{ nm}$ . As for bilayer and 3–4 layer graphene, the height are  $3.5\text{ nm}$  and

6 nm, respectively. The AFM data of monolayer graphene in solution phase is much higher than that of clean and pristine graphene ( $\sim 0.4$  nm) because too much surfactant and solvent molecules absorbing on graphene surface or between graphene and silicon wafer. In our work, delamination of graphene from Cu powder is achieved in solution phase and no surfactant is applied. Therefore, the layer number of graphene in our work is no more than 5, which is consistent with the results of Raman spectra.

## Conclusion

We demonstrate a simple method to produce CVD-grown, multilayer graphene on Cu powder. Graphite is added to isolate Cu powder from sintering, and Cu powder with graphene could be separated by the water/hexane interface. The graphene composed of multilayer carbon atom sheets ( $< 5$  layers) from electrochemical delamination is proven by Raman spectra and AFM images. The Cu powder as a substrate for CVD growth could be maintained and reused in multiple growths and delamination cycles.

## Acknowledgements

This research is sponsored by NASA Glenn Research Center under contract No. NNX14CS53P, and the Special Fund for Basic Scientific Research of Central Colleges, Chang'an University, No. CHD2010JC053.

## References

- 1 A. K. Geim, Graphene: status and prospects, *Science*, 2009, **324**, 1530–1534.
- 2 Y. B. Zhang, Y. W. Tan, H. L. Stormer, *et al.*, Experimental observation of the quantum Hall effect and Berry's phase in graphene, *Nature*, 2005, **438**, 201–204.
- 3 F. Schwierz, Graphene transistors, *Nat. Nanotechnol.*, 2010, **5**, 487–496.
- 4 (a) X. S. Li, W. W. Cai, J. An, *et al.*, Large-area synthesis of high-quality and uniform graphene films on copper foils, *Science*, 2009, **324**, 1312–1314; (b) K. S. Kim, Y. Zhao, H. Jang, *et al.*, Large-scale pattern growth of graphene films for stretchable transparent electrodes, *Nature*, 2009, **457**, 706–710.
- 5 W. A. de Heer, C. Berger, X. S. Wu, *et al.*, Epitaxial graphene, *Solid State Commun.*, 2007, **143**, 92–100.
- 6 H. M. Hwang, P. Joo, M. S. Kang, *et al.*, Highly tunable charge transport in layer-in-layer assembled graphene transistors, *ACS Nano*, 2012, **6**, 2432–2440.
- 7 N. I. Kovtyukhova, P. J. Ollivier, B. R. Martin, *et al.*, Layer-by-layer assembly of ultrathin composite films from micron-sized graphite oxide sheet and polycations, *Chem. Mater.*, 1999, **11**, 771–778.
- 8 Z. Xu and C. Gao, Aqueous liquid crystals of graphene oxide, *ACS Nano*, 2011, **5**, 2908–2915.
- 9 V. C. Tung, M. J. Allen, Y. Yang, *et al.*, High-throughput solution processing of large-scale graphene, *Nat. Nanotechnol.*, 2009, **4**, 25–29.
- 10 Y. Hernandez, V. Niclosi, M. Lotya, *et al.*, High-yield production of graphene by liquid-phase exfoliation of graphite, *Nat. Nanotechnol.*, 2008, **3**, 563–568.
- 11 Z. F. Wang, J. J. Liu, W. X. Wang, *et al.*, Aqueous phase preparation of graphene with low defect density and adjustable layers, *Chem. Commun.*, 2013, **49**, 10835–10837.
- 12 C. Mattevi, H. Kim and M. Chhowalla, A review of chemical vapor deposition of graphene on copper, *J. Mater. Chem.*, 2011, **21**, 3324–3334.
- 13 Y. Lee, S. Bae, H. Jang, *et al.*, Wafer-scale synthesis and transfer of graphene films, *Nano Lett.*, 2010, **10**, 490–493.
- 14 Y. Wang, Y. Zheng, X. Xu, *et al.*, Electrochemical delamination of CVD-grown graphene film: toward the recyclable use of copper catalyst, *ACS Nano*, 2011, **5**, 9927–9933.
- 15 L. B. Gao, W. C. Ren, H. L. Xu, *et al.*, Repeated growth and bubbling transfer of graphene with millimeter-size single crystal grains using platinum, *Nat. Commun.*, 2012, **3**, 699.
- 16 J. Rafiee, X. Mi, H. Gullapalli, *et al.*, Wetting transparency of graphene, *Nat. Mater.*, 2012, **11**, 217–222.
- 17 J. N. Coleman, Liquid-phase exfoliation of nanotubes and graphene, *Adv. Funct. Mater.*, 2009, **19**, 3680–3695.
- 18 J. Israelachvili, *Intermolecular and Surface Forces*, Academic Press, London, 2nd edn, 1991.
- 19 P. de Gennes, *Capillarity and Wetting Phenomena*, Springer, New York, 2003.
- 20 C. Bondy and K. Sollner, On the mechanism of emulsification by ultrasonic waves, *Trans. Faraday Soc.*, 1935, **31**, 835–843.
- 21 T. G. Mason, J. N. Wilking, K. Meleson, *et al.*, Nanoemulsions: formation, structure, and physical properties, *J. Phys.: Condens. Matter*, 2006, **18**, 635–666.
- 22 B. P. Binks and S. O. Lumsdon, Influence of particle wettability on the type and stability of surfactant-free emulsions, *Langmuir*, 2000, **16**, 8622–8631.
- 23 G. Hameeda, M. K. Baloch, M. Nawaz, *et al.*, Impact of intensity of ultrasonication on the properties of *n*-hexane–water emulsion, *Russ. J. Phys. Chem. A*, 2011, **85**, 792–796.
- 24 X. L. Liang, B. A. Sperling, I. Calizo, *et al.*, Toward clean and crackles transfer of graphene, *ACS Nano*, 2001, **5**, 9144–9153.
- 25 C. J. L. de la Rosa, J. Sun, N. Lindvall, *et al.*, Frame assisted H<sub>2</sub>O electrolysis induced H<sub>2</sub> bubbling transfer of large area graphene grown by chemical vapor deposition on Cu, *Appl. Phys. Lett.*, 2013, **102**, 022101.
- 26 A. C. Ferrari, J. C. Meyer, V. Scardaci, *et al.*, Raman spectrum of graphene and graphene layers, *Phys. Rev. Lett.*, 2006, **97**, 187401.
- 27 A. C. Ferrari and D. M. Basko, Raman spectroscopy as a versatile tool for studying the properties of graphene, *Nat. Nanotechnol.*, 2013, **8**, 235–246.
- 28 C. J. Shih, A. Vijayaraghavan, R. Krishnan, *et al.*, Bi- and trilayer graphene solutions, *Nat. Nanotechnol.*, 2011, **6**, 439–445.